

Candidate neutrino-emitting blazars sharing physical properties with TXS 0506+056

Ilaria Viale,^{a,*} C. Righi,^b G. Principe,^c M. Cerruti,^d F. Tavecchio^b and E. Bernardini^a on behalf of the Fermi/LAT Collaboration

^aUniversity of Padova and INFN, I-35131 Padova, Italy

^bNational Institute for Astrophysics (INAF), I-00136 Rome, Italy

^cUniversity of Trieste and INFN, I-34127 Trieste, Italy

^dUniversité Paris Cité, CNRS, Astroparticule et Cosmologie, F-75013 Paris, France

E-mail: ilaria.viale.1@phd.unipd.it

Blazars are highly energetic objects with a broad band emission covering the whole electromagnetic spectrum. Their spectral energy distribution can be described in terms of both hadronic and leptonic processes. In leptonic models the emission is produced by electrons and positrons in the relativistic jet, while in hadronic ones the contribution from accelerated protons becomes relevant. Importantly, only hadronic processes allow the production of high energy neutrinos, the detection of which is an important step towards finding the long-sought sources of ultra-high energy cosmic rays. Among the potential neutrino-emitter candidates, the interest in blazars has grown after the evidence for a joint photon-neutrino emission from the gamma-ray flaring source TXS 0506+056 in 2017. Since the possible emission of neutrinos from TXS 0506+056 is not fully understood, it is important to investigate the emission properties of sources with similar features. In this work, we scan the most recent 4LAC-DR2 Fermi catalog, based on 10 years of Fermi-LAT data, searching for other sources sharing similar properties as TXS 0506+056. The selection of candidates is made by focusing on a number of key parameters, which were constrained in a range close to the TXS 0506+056 value. The efficiency of the accretion mechanism and the nature of the candidates as Flat Spectrum Radio Quasars or BL Lac objects is analyzed. Furthermore, potential information on the neutrino flux from these sources and the detectability prospects at TeV energies are investigated via a lepto-hadronic modeling of their spectral energy distribution.

38th International Cosmic Ray Conference (ICRC2023)
26 July - 3 August, 2023
Nagoya, Japan



*Speaker

1. Introduction

The existence of high-energy neutrinos of cosmic origin was announced by the IceCube Neutrino Observatory in 2013 [1] and is now well established. High-energy astrophysical neutrinos are thought to be produced in the interactions of accelerated cosmic-rays with ambient matter or radiation fields, providing a smoking gun of hadronic interactions. Within the potential neutrino sources blazars are interesting candidates. They are a subclass of Active Galactic Nuclei (AGN) hosting a relativistic jet pointing very close to the observer's line of sight ($< 10^\circ$), which provides a favorable environment for particle acceleration, protons included, and neutrino production through photomeson interactions. This was supported by the multi-messenger observation of photon and neutrino emission from the flaring blazar TXS 0506+056 in 2017 [2], representing the first evidence for a neutrino source. However, despite the many models developed to describe this multi-messenger observation, neutrino emission from TXS 0506+056 is still not fully understood. Indeed, taking into account the two subclasses of blazars – Flat Spectrum Radio Quasars (FSRQ) and BL Lac objects (BL Lac) – this source appears not to be a pure BL Lac, nor a pure FSRQ. It was initially classified as a BL Lac, but a possible FSRQ nature was suggested by [3]. Moreover, this source is placed in the middle of the blazar sequence, a work developed by [4] which identified different properties of the two blazar subclasses related to their broad-band Spectral Energy Distribution (SED). Its placement in the blazar sequence could suggest transitional properties between the two subclasses.

In this contribution we select a sample of blazars sharing similar properties of TXS 0506+056 aiming at investigating their nature as BL Lacs or FSRQs through an evaluation of the efficiency of their accretion mechanism. Indeed, FSRQs are thought to have an efficient accretion disk and a Broad Line Region (BLR) rich of ionized material, while BL Lacs are thought to be less powerful than FSRQs, with a probably inefficient disk and a poor or absent BLR [5]. In addition, simultaneous multiwavelength data from the selected sources are analyzed and their broad-band SED modeled in a context of lepto-hadronic emission in order to predict the potential neutrino flux from these objects and the detectability prospect at very high energies (VHE). We concentrate our discussion on one of the selected candidates.

2. Selection of candidates

We selected the sources from the second release of the Fourth Catalog of Active Galactic Nuclei (4LAC-DR2, [6, 7]), based on the first 10 years of Fermi/LAT observations, from August 2008 to August 2018. Taking into account the typical shape of the spectral energy distribution of blazars and the results arising from the study on the blazar sequence [4], we based the selection on three main parameters, aiming at selecting sources governed by the same physical mechanisms. In particular, the parameters considered for the selection are: the γ -ray photon index, the integral luminosity in the 1 – 100 GeV energy range and the frequency of the synchrotron peak. The first and the last parameters are taken directly from the 4LAC-DR2 catalog, while the integral luminosity was computed according to [8], starting from the Fermi flux reported in the 4LAC-DR2 and the source redshift¹. We selected all the sources with parameters values close to TXS 0506+056 ones,

¹Note that all sources without a known redshift could not be considered in the selection.

Table 1: Final sample of sources with information on redshift and emission lines. The columns are: source name, associated counterpart name, redshift found in the literature, emission lines observed in the optical spectrum, luminosity of each line, references.

Source	Alias	z_{ref}	Emission lines	L_{lines} [$10^{41} \text{ erg s}^{-1}$]	Refs
4FGL J0509.4+0542	TXS 0506+056	0.3365	[O II]	1.0	[9, 10]
			[O III]	0.05	
			[N II]	0.05	
4FGL J0050.7-0929	PKS 0048-09	0.635	[O II]	1.0	[10]
			[O III]	0.94	
			H α	1.6	
4FGL J1309.4+4305	B3 1307+433	0.693	[O II]	20.0	[10]
			[O III]	5.5	
4FGL J0114.8+1326	GB6 J0114+1325	0.685	H β	124	[11]
			[O III]	245	

in particular: $\Gamma_{\gamma} \in (\Gamma_{\gamma, \text{TXS}} - 0.5, \Gamma_{\gamma, \text{TXS}} + 0.5)$, $\log_{10} L_{\gamma} \in (\log_{10} L_{\gamma, \text{TXS}} - 0.5, \log_{10} L_{\gamma, \text{TXS}} + 0.5)$, $\log_{10} \nu_S \in (\log_{10} \nu_{S, \text{TXS}} - 0.7, \log_{10} \nu_{S, \text{TXS}} + 0.7)$, where $\Gamma_{\gamma, \text{TXS}} = 2.079 \pm 0.014$, $\nu_{S, \text{TXS}} = 3.55 \times 10^{14} \text{ Hz}$ and $L_{\gamma, \text{TXS}} = (1.62 \pm 0.04) \times 10^{46} \text{ erg/s}$ are the values related to TXS 0506+056. From this first selection a sample of 27 sources arised, the majority of which are BL Lacs.

For each source we inspected the reliability of the redshift value reported in the catalog through a search in the literature and performed a further selection aimed at keeping only those sources showing an established redshift and a detailed spectral analysis showing information on their emission lines. The sample resulting from this selection consists of 4 sources, including TXS 0506+056, all classified as BL Lacs. Information on their redshift and spectral lines are reported in Table 1.

3. Estimation of accretion rate

The information provided by the spectral analysis of the candidates can be exploited in two ways mainly. On the one hand, they are essential to put constraints on some parameters of the modeling such as the energy density of photons from the BLR, the computation of which will be shown in Sec. 5. On the other hand they can provide information on the accretion flow of the objects, which gives a hint about their nature as BL Lacs or FSRQs [5]. In this section we give an estimation of the latter quantity.

The efficiency of the accretion flow of an AGN can be quantified through the computation of the accretion rate, a quantity describing the amount of matter accreted by the black hole in the unit of time and given by $\dot{M} = L_{\text{disk}}/(\eta c^2)$, where L_{disk} is the luminosity of the accretion disk and η parametrizes the amount of accretion energy being radiated. The luminosity of the disk is directly related to the luminosity of the BLR, in turn linked to the luminosity of the emission lines, since the broad emission lines observed in the optical spectrum of an AGN come from the plasma directly ionized by the disk radiation. Thus, we can give an estimation of the BLR luminosity starting from the information on the spectral lines reported in the previous section. In particular,

Table 2: Estimated values of BLR luminosity, disk luminosity and accretion rate.

Source	L_{BLR} [erg s ⁻¹]	L_{disk} [erg s ⁻¹]	\dot{m}_{low}	\dot{m}_{high}
TXS 0506+056	2.55×10^{43}	2.55×10^{44}	1.96×10^{-3}	1.96×10^{-2}
PKS 0048-09	2.42×10^{42}	2.42×10^{43}	1.86×10^{-4}	1.86×10^{-3}
B3 1307+433	3.39×10^{44}	3.39×10^{45}	2.61×10^{-2}	2.61×10^{-1}
GB6 J0114+1325	3.66×10^{44}	3.66×10^{45}	2.82×10^{-2}	2.82×10^{-1}

we follow Eq. 1 of [12]: $L_{\text{BLR}} = \sum_i L_{i,\text{obs}} \frac{\langle L_{\text{BLR}}^* \rangle}{\sum_i L_{i,\text{est}}}$, where $L_{i,\text{obs}}$ is the observed luminosity, $L_{i,\text{est}}$ is the line ratio, namely the line luminosity with respect to the Ly α line as reported in Table 1 of [13], and $\langle L_{\text{BLR}}^* \rangle$ is the sum of the ratios. The disk luminosity was then estimated by assuming that the radiation reprocessed by the BLR is about 10% of the whole disk emission. From here, the accretion rate in units of the Eddington luminosity, $\dot{m} = L_{\text{disk}}/L_{\text{Edd}}$, was computed, where the Eddington luminosity is $L_{\text{Edd}} = 1.3 \times 10^{38} \frac{M}{M_{\odot}} \frac{\text{erg}}{\text{s}}$. Since the precise value of the black hole mass is not known for the selected objects, we assumed two possible values bracketing the BH mass distribution, $M_{\text{BH}} = 10^8, 10^9 M_{\odot}$, in order to define a possible range where \dot{m} can lie. The values obtained for each source are reported in table 2.

As we can see, although selection was based on similar properties, the results obtained suggest a different behaviour. Indeed, if we take into account the division proposed by [5], considering as FSRQs the sources with \dot{m} above the critical value $\dot{m}_c \sim 5 \times 10^{-3}$, and as BL Lacs the ones with $\dot{m} < \dot{m}_c$, we can see that an efficient accretion regime is suggested for B3 1307+433 and GB6 J0114+1325, while an inefficient one for PKS 0048-09. For TXS 0506+056 we cannot draw a conclusion since the recovered accretion rate range lies around \dot{m}_c .

4. Multiwavelength data analysis

In this work we are interested in identifying high and low states of activity where simultaneous MWL observations are performed in order to build consistent SEDs and emission models. In order to do this, we analyzed public multiwavelength data from Swift and Fermi observatories. For each source, we built the long-term lightcurve, in order to identify eventual high states of activity and quiescent ones, and simultaneous SEDs on the selected periods. However, all the selected sources have a quite poor long-term Swift coverage and only PKS 0048-09 shows signs of flaring activity. Thus, we selected a high and quiescent state for this source, while we concentrated just on the quiescent one for the others. Note that for this source the high state only includes an increased flux in UV and γ -rays, while in X-rays it resulted in a quiescent state (see [14]). In the following we report a brief description of the Swift and Fermi satellites and the analysis methods used. The SEDs comprising both analyzed and archival data for each source in the selected periods are shown in Fig. 1.

4.1 Swift/XRT, UVOT

The *Neil Gehrels Swift observatory* satellite [15] is multiwavelength mission equipped with 3 instruments sensitive to the ultraviolet and X-ray bands. We used data from the X-ray telescope

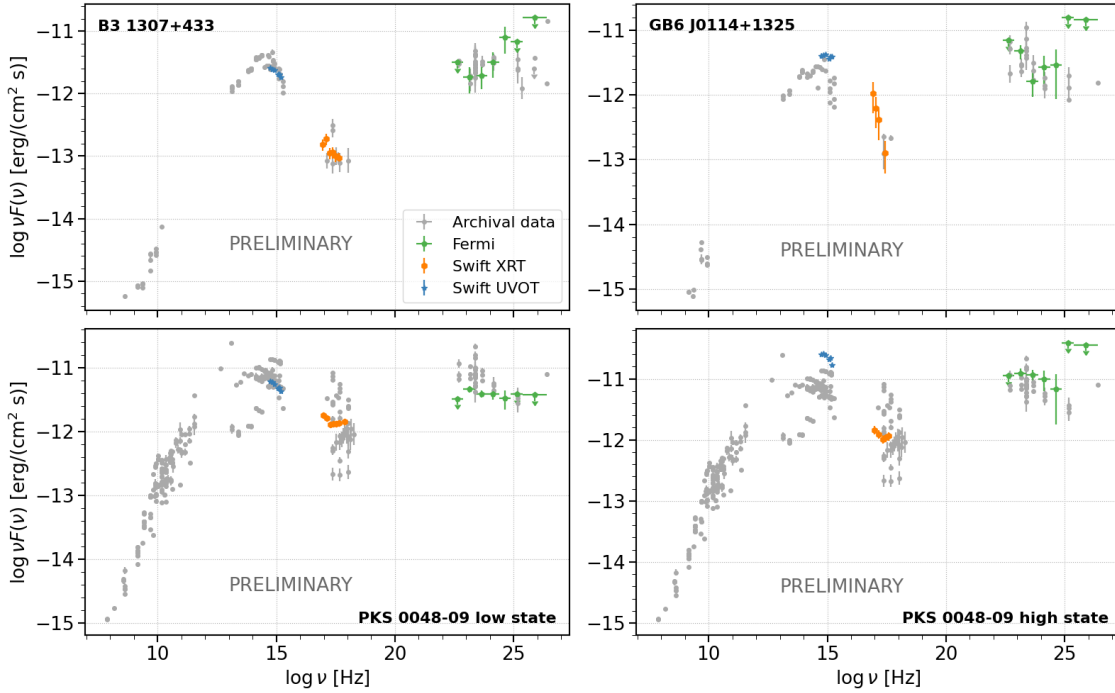


Figure 1: Spectral energy distribution of the selected candidates. Grey points correspond to archival data from ASI SSDC², while blue, orange and green points are simultaneous Swift/UVOT, Swift/XRT and Fermi/LAT data corresponding to the selected periods, respectively.

(XRT, 0.2 – 10 keV) [16] and the Ultraviolet/Optical Telescope (UVOT, 170 – 600 nm) [17]. The XRT observations were performed in photon counting mode [18] and each spectrum was rebinned in order to have at least 20 – 30 counts per bin in order to apply the χ^2 statistic. When this was not possible, the Cash statistic was used [19]. The UVOT observations were performed using all the six filters on board the UVOT module (v , b , u , $w1$, $m2$, $w2$) and differential photometry was applied to recover the magnitude of the sources. Results were then corrected for galactic extinction [20].

4.2 Fermi/LAT

The Large Area Telescope on board the Fermi satellite is a pair conversion telescope with a energy range from 20 MeV to more than 300 GeV [21]. We analyzed 12 years of P8R3 source class data between 100 MeV and 1 TeV in a region of interest of $15^\circ \times 15^\circ$ centered on the source location. Events with a zenith angle $Zd > 105^\circ$ were cut in order to reduce the contamination from background γ -ray events from the Earth limb. The analysis was performed using Fermipy [22] (<https://arxiv.org/abs/1707.09551>) and adopting the same spectral function used in the 4LAC-DR2.

5. Modeling

The multi-messenger emission of TXS 0506+056 during the 2017 campaign was explained in terms of a lepto-hadronic scenario where the high energy bump of the SED has a predominantly

²<https://www.ssdsc.asi.it/>

Table 3: Fit results for model of B3 1307+433. Primed quantities refer to the jet reference frame.

B3 1307+433		B3 1307+433	
z	0.69	$\gamma'_{e,min}$	300
δ	30	$\gamma'_{e,break}$	2200
B [G]	1	$\gamma'_{e,Max}$	15000
R [cm]	1.25×10^{16}	$\alpha_{e,1}$	2.0
$\gamma'_{p,min}$	1	$\alpha_{e,1}$	3.5
$\gamma'_{p,Max}$	10^8	N_e [cm $^{-3}$]	800
α_p	2.0	$u'_{ph,BLR}$ [erg cm $^{-3}$]	0.2
N_p [cm $^{-3}$]	56	$u'_{ph,torus}$ [erg cm $^{-3}$]	0.028

leptonic origin, given by the inverse Compton scattering of soft photons by primary electrons. The hadronic component is also present but with a minor contribution. It explains the X-ray and VHE γ -ray emission of the source through photo-meson interactions and Bethe-Heitler pair production.

In this section we present the modeling of the source B3 1307+433 under the same framework, using the same LeHa [23] code used for TXS 0506+056. However, given our results in Sec. 3, we expect an efficient accretion and a rich BLR from this source, so we decided to take into account the contribution from the BLR on external Compton. In this context, an important parameter is the radiation energy density of the broad emission line photons, which can be recovered thanks to our study on the spectral lines presented in Sec. 3. This quantity depends on the luminosity and radius of the BLR, L_{BLR} and R_{BLR} respectively. The former has already been estimated and is reported in Table 2, while the latter can be estimated by assuming a simple scaling relation with the disk luminosity (also reported in Table 2): $R_{BLR} = 10^{17} L_{disk,45}^{1/2}$ cm [24], where $L_{disk,45}^{1/2}$ is the luminosity of the disk in units of 10^{45} erg s $^{-1}$. The photon energy density is then given by $u_{ph,BLR} = \frac{L_{BLR}}{4\pi c R_{BLR}^2} 2.24$. The results obtained for B3 1307+433 are: $R_{BLR} = 1.84 \times 10^{17}$ cm, $u_{ph,BLR} = 5.95 \times 10^{-2}$ erg cm $^{-3}$. A similar procedure can be applied to estimate the radius and luminosity of the torus, whose contribution is considered in the external Compton too. Assuming that the torus reprocesses $\sim 40\%$ of the disk radiation and the scaling relation $R_{torus} = 2.5 \times 10^{18} L_{disk,45}^{1/2}$ [24], we obtain $L_{torus} = 0.4 L_{disk} = 1.36 \times 10^{45}$ erg s $^{-1}$, $R_{torus} = 4.60 \times 10^{18}$ cm and $u_{ph,torus} = 3.81 \times 10^{-4}$ erg cm $^{-3}$.

In the model, the photon distribution of the BLR is considered as a delta function, assuming that the whole BLR emission is dominated by the $1y\alpha$ line, while for the torus we assume a black body with temperature $T = 420$ K. These quantities are kept free while building the model and then compared to the predicted values. The model of B3 1307+433 SED is shown in Fig. 2, while the fit results are reported in Table 3.

6. Conclusion and outlook

In this contribution we selected candidate neutrino emitters based on specific parameters of their SED, constrained to be similar to the ones of TXS 0506+056. From an initial selection of 27 sources, only 4 objects could be considered since they were the only ones showing an established redshift and a detailed spectral analysis, which represent an essential point of this work. This fact

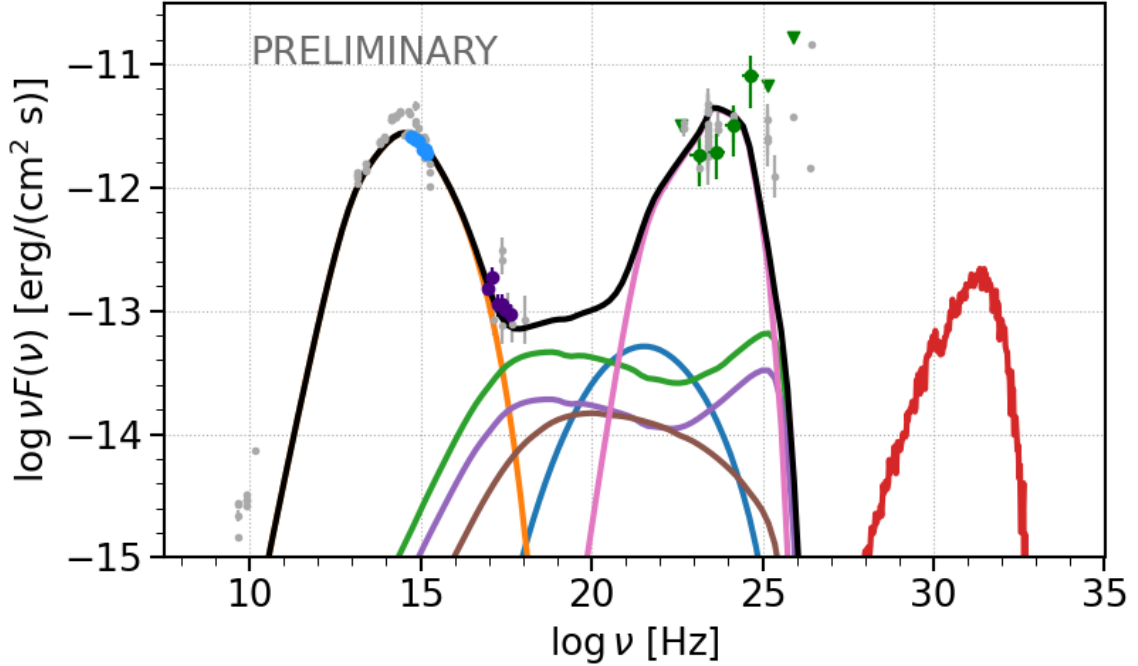


Figure 2: Modeling of the SED of B3 1307+433. The spectral points are defined as in Fig. 1, the lines represent synchrotron emission from relativistic electrons (orange), external Compton emission from both the BLR and the torus (pink), synchrotron self Compton process (blue), cascades from π^0 decay, cascades from π^\pm decay (violet), cascades from Bethe-Heitler process (brown), and all-flavour neutrino spectrum (red).

highlights the importance and need to perform spectroscopic studies of these objects, which would be highly beneficial to enlarge the number of candidates in the sample.

For each candidate the accretion rate and the photon energy density of the BLR and torus were estimated starting from information on their spectral lines. Results suggest a different nature for these sources. Indeed, the selected candidates may be powered by different physical mechanisms given the different values found for the accretion rates. For PKS 0048-09 we obtained $\dot{m} \in (1.86 \times 10^{-4}, 1.86 \times 10^{-3})$, suggesting an inefficient accretion flow and a poor BLR, while for B3 1307+433 and GB6 J0114+1325 we obtained $\dot{m} \in (2.61 \times 10^{-2}, 2.61 \times 10^{-1})$ and $\dot{m} \in (2.82 \times 10^{-2}, 2.82 \times 10^{-1})$ respectively, suggesting an efficient accretion flow and a BLR rich of gas. Further studies on these sources are then needed to confirm their nature as BL Lacs or FSRQs.

Finally, we presented a lepto-hadronic modeling of B3 1307+433 SED based on the one used to describe TXS 0506+056 emission during the 2017 campaign but taking into account different target photon fields for external Compton emission, namely the photons from BLR and torus. This model attributes the high-energy bump of the SED to the mentioned leptonic component. However, in this band, the analyzed Fermi/LAT data show a hard spectrum with a peak possibly around 10^{25} Hz which is well fitted by a log-parabola [6, 7], while the model shown here predicts a lower peak frequency. The hadronic contribution is instead suggested in the X-ray band, specifically in the synchrotron emission tail, and in the VHE γ -ray band. In both ranges it mainly consists of cascades resulting from photo-meson interactions and, in the first case, it connects the low- and high-energy

bumps of the spectrum. Detailed results for all sources will be presented in an upcoming paper.

Acknowledgements

The *Fermi*-LAT Collaboration acknowledges support from NASA and DOE (United States), CEA/Irfu, IN2P3/CNRS, and CNES (France), ASI, INFN, and INAF (Italy), MEXT, KEK, and JAXA (Japan), and the K.A. Wallenberg Foundation, the Swedish Research Council, and the National Space Board (Sweden).

References

- [1] Aartsen, M. G., Ackermann, M., Adams, J., et al., *JINST* **12** (2017), P03012
- [2] The IceCube Collaboration et al., *Science* **361** eaat1378 (2018)
- [3] Padovani P., et al., *MNRAS*, **484** (2019), L104
- [4] Ghisellini G., Righi C., Costamante L., Tavecchio F., *MNRAS*, **469** (2017), 255
- [5] Ghisellini G., Tavecchio F., Foschini L., Ghirlanda G., *MNRAS*, **414** (2011), 2674
- [6] Ajello M., et al., *ApJ*, **892** (2020), 105
- [7] Lott B., Gasparri D., Ciprini S., 2020, arXiv e-prints, p. arXiv:2010.08406
- [8] Ghisellini G., Maraschi L., Tavecchio F., *MNRAS: Letters*, **396** (2009), L105
- [9] Paiano S., Falomo R., Treves A., Scarpa R., *ApJ*, **854** (2018), L32
- [10] Landoni M., Falomo R., Paiano S., Treves A., *ApJS*, **250** (2020), 37
- [11] Shaw M. S., et al., *ApJ*, **748** (2012), 49
- [12] Celotti A., Padovani P., Ghisellini G., *MNRAS*, **286** (1997), 415
- [13] Francis P. J., et al., *ApJ*, **373** (1991), 465
- [14] Viale I. et al., in preparation
- [15] Gehrels N., et al., *ApJ*, **611** (2004), 1005
- [16] Burrows D. N., et al., *Space Sci. Rev.*, **120** (2005), 165
- [17] Roming P. W. A., et al., *Space Sci. Rev.*, **120** (2005), 95
- [18] Hill J. E., et al., *Proc. SPIE Conference Series*, **5165** (2004), 217
- [19] Cash W., *ApJ*, **228** (1979), 939
- [20] Roming P. W. A., et al., *ApJ*, **690** (2009), 163
- [21] Atwood W. B., et al., *ApJ*, **697** (2009), 1071
- [22] Wood M., et al., arXiv e-prints, p. arXiv:1707.09551
- [23] Cerruti M., Zech A., Boisson C., Inoue S., *MNRAS*, **448** (2015), 910
- [24] G. Ghisellini, F. Tavecchio, *MNRAS*, **387** (2008), 1669